

A&A manuscript no.

(will be inserted by hand later)

Your thesaurus codes are:

08.05.1, 08.23.2, 09.04.1, 09.08.1, 09.09.1, 09.11.1, 11.09.1, 11.13.1

ASTRONOMY
AND
ASTROPHYSICS

HST observations of the very young SMC “blob” N 88A^{*, **}

M. Heydari-Malayeri¹, V. Charmandaris¹, L. Deharveng², M.R. Rosa^{3, ***}, and H. Zinnecker⁴¹ DEMIRM, Observatoire de Paris, 61 Avenue de l’Observatoire, F-75014 Paris, France² Observatoire de Marseille, 2 Place Le Verrier, F-13248 Marseille Cedex 4, France³ Space Telescope European Coordinating Facility, European Southern Observatory, Karl-Schwarzschild-Strasse-2, D-85748 Garching bei München, Germany⁴ Astrophysikalisches Institut Potsdam, An der Sternwarte 16, D-14482 Potsdam, Germany

Received 27 January 1999 / Accepted 20 April 1999

Abstract. High-resolution *Hubble Space Telescope* images have allowed us for the first time to resolve the compact SMC ionized “blob” N 88A (diameter $\sim 3''.5$ or 1 pc). This very young H II region, which is hatching from its natal molecular cloud, is heavily affected by absorbing dust associated with the cloud. The interstellar reddening towards N 88A is on average $A_V \sim 1.5$ mag and strikingly rises to more than 3.5 mag in a narrow dust band crossing the core of the H II region. Such a high extinction is unprecedented for an H II region in the metal-poor SMC. We present the photometry of some 70 stars lying towards the OB association at the center of which lies N 88A. The exciting star(s) of N 88A is not detected, due to the heavy extinction. The chronology of star formation is discussed for the whole region.

Key words: Stars: early-type – dust, extinction – H II regions – individual objects: N 88 – Galaxies: Magellanic Clouds

1. Introduction

The *Hubble Space Telescope* (*HST*) offers a unique opportunity for studying very young massive star formation regions in the outer galaxies. The fact that the Small Magellanic Cloud (SMC) is the most metal-poor galaxy observable with very high angular resolution makes it an ideal laboratory for investigating star formation in very distant galaxies reminiscent of those populating the early Universe.

Send offprint requests to: M. Heydari-Malayeri, heydari@obspm.fr

* Based on observations with the NASA/ESA Hubble Space Telescope obtained at the Space Telescope Science Institute, which is operated by the Association of Universities for Research in Astronomy, Inc., under NASA contract NAS5-26555.

** Based on observations obtained at the European Southern Observatory, La Silla, Chile.

*** Affiliated to the Astrophysics Division, Space Science Department of the European Space Agency.

Our search for the youngest massive stars in the Magellanic Clouds started almost two decades ago on the basis of ground-based observations. This led to the discovery of a distinct and very rare class of H II regions in these galaxies, that we called high-excitation compact H II “blobs” (HEBs). So far only five HEBs have been found in the LMC: N 159-5, N 160A1, N 160A2, N 83B-1, and N 11A (Heydari-Malayeri & Testor 1982, 1983, 1985, 1986, Heydari-Malayeri et al. 1990) and two in the SMC: N 88A and N 81 (Testor & Pakull 1985, Heydari-Malayeri et al. 1988a). These objects are expected to harbor newborn massive stars.

The first part of our *HST* project studying the H II “blobs” was devoted to the SMC N 81 (Heydari-Malayeri et al. 1999, hereafter Paper I). The Wide Field Planetary Camera 2 (WFPC2) observations allowed us to resolve N 81 and discover a tight cluster of newborn massive stars embedded in this nebula of $\sim 10''$ across. The WFPC2 images also uncovered a striking display of violent phenomena such as stellar winds, shocks, and ionization fronts, typical of turbulent starburst regions.

The SMC “blob” N 88A is part of the H II region N 88 (Henize 1956), or DEM 161 (Davies et al. 1976) which lies in the Shapley Wing at $\sim 2^\circ 2'$ (2.4 kpc) from the main body of the SMC. Other H II regions lying towards the Wing are from west to east N 81, N 84, N 89, and N 90. The HEB nature of N 88A was first recognized by Testor and Pakull (1985) who used CCD imaging at $\sim 2''$ resolution through H α , H β , and [O III] filters and IDS spectroscopy ($4'' \times 4''$ aperture) to study the central component N 88A. They found a high excitation object ([O III]/H β = 7.8) with an interstellar extinction $A_V = 1.7$ mag. The chemical abundances in N 88 had previously been determined by Dufour & Harlow (1977) who, using a $10'' \times 79''$ slit, found a low-metal content typical of the chemical composition of the SMC. CCD photometry and spectroscopy of 10 stars lying around N 88A were carried out by Wilcots (1994) using the CTIO 90 cm telescope. However, the ground-based observations in general were unable to reveal the internal morphology and stellar content of N 88A.

The *HST* was used for imaging and FOS spectroscopy of N 88A (Kurt et al. 1995). These pre-COSTAR observations, in spite of the effort made in data analysis, could not clearly show the internal details of N 88A. Garnett et al. (1995) revisited the chemical abundances in N 88A on the basis of *HST* ultraviolet FOS ($0''.7 \times 2''.0$ aperture) and ground-based spectra.

In this paper we present recent *HST* observations (GO 6535) of N 88A and its surroundings. In the following sections we elaborate on the extinction and emission properties of each component and suggest a plausible scenario on the star formation history of this region.

2. Observations and data reduction

The observations of N 88A described in this paper were obtained with WFPC2 on board the *HST* on August 31, 1997 using the wide- and narrow-band filters (F300W, F467M, F410M, F547M, F469N, F487N, F502N, F656N). The observational techniques, data reduction procedures, and photometry are similar to those explained in detail in Paper I. A composite image is presented in Fig. 1.

The ESO EFOSC Camera at the 3.6 m telescope was also used on 4 June 1988 for imaging N 88 through a narrow $H\alpha$ filter (ESO#507, λ 6565.5 Å, $\Delta\lambda = 12$ Å) with exposure times of 1 and 5 minutes. The detector was a RCA CCD chip (#11) with $0''.36$ pixels and the seeing was $\sim 1''.5$ (FWHM). This $H\alpha$ image is displayed in Fig. 2. Due to its relatively short exposure, this image displays only the brightest part of the H II emission.

3. Results

3.1. Morphology

N 88 is a relatively large concentration of ionized gas with several components (Fig. 1a). From the central region emanate a number of fine-structure filaments running southwards over $40''$ (~ 10 pc) which can be seen in the “true-color” composite image (Fig. 1a). The larger field of the $H\alpha$ image obtained with EFOSC (Fig. 2) shows a veil of thin filaments curling southwards over more than 20 pc and brightening at some points.

The main component, N 88A, is a compact, high excitation H II region $\sim 3''.5$ (~ 1 pc) in diameter surrounded by seven diffuse H II regions, labelled B to H in Fig. 1b. N 88A has a complex morphology. An absorption lane crossing the nebula from north to south appears as an undulating yellow structure in Fig. 1c (see Sect. 3.2 for more details). West of this structure lies the brightest part of N 88A, a small core of diameter $\sim 0''.3$ (0.08 pc), especially apparent on the $H\alpha$ image (white spot in Fig. 1c; see also Fig. 5). N 88A is clearly ionization-bounded to the north-west since the sharp edge visible in Fig. 1 indicates an ionization front in that direction. It is limited to the south-east by the weaker component B. N 88B resembles a hollow sphere – a shell – centered on the bright star #55

(see Sect. 3.4). N 88A and N 88B are clearly in interaction, as shown by the brightening of the shell between the two regions. Moreover, we note a high excitation narrow filament showing up in the [O III] emission north-east of N 88B (Fig. 1a). The other components are situated farther away from N 88A. N 88 E-F-G and H appear as more extended, diffuse, and spherical H II regions.

Several lower excitation arc-shaped features and filaments emerging from N 88A run outward in the north-east and south-west directions. These wind-induced structures are best seen in Fig. 3, which presents an un-sharp masked image of N 88A-B created from $H\alpha$. In this image large-scale structures have been suppressed by the technique explained in Paper I. Note also the mottled structure of the main component A, even in the direction of the absorbing lane, indicating a very inhomogeneous medium, both for gas and dust, with a typical cell size of $0''.4$ (0.1 pc).

3.2. Nebular reddening

The Balmer $H\alpha/H\beta$ intensity ratio map of N 88A-B is presented in Fig. 4a. The most striking feature is the presence of a heavy absorption lane of $\sim 0''.7 \times 2''.3$ ($\sim 0.2 \times 0.7$ pc²) in size, running in a north-south direction, which divides the bright N 88A into two parts. The mean $H\alpha/H\beta$ ratio in the lane is 7.10 ± 1.42 (rms), corresponding to $A_V = 2.5$ mag if the LMC interstellar reddening law is used (Prévot et al. 1984), and reaches values as high as ~ 10 , or $A_V \sim 3.5$ mag. The mean ratio for component A, 4.81 ± 1.46 , corresponds to $A_V \sim 1.5$ mag. The extinction is also high towards component B, where $H\alpha/H\beta$ keeps a relatively uniform value of 4.27 ± 0.90 ($A_V \sim 1.1$ mag). For comparison, previous lower resolution spectroscopic observations yielded $A_V = 1.1$ mag (Dufour & Harlow 1977, using a $10''$ wide slit) and $A_V = 1.7$ mag (Testor & Pakull 1985, $4'' \times 4''$ slit). The $H\alpha/H\beta$ map was used to de-redden the $H\beta$ flux on a pixel to pixel basis.

The G component shows a sharp dividing line in the middle separating it into two distinct halves, one much fainter than the other. This feature should be due to absorbing dust.

3.3. Ionized gas emission

The total $H\beta$ flux of component A is $F(H\beta) = 3.45 \times 10^{-12}$ erg s⁻¹ cm⁻² (accurate to $\sim 3\%$). Correcting for the reddening (Sect. 3.2) gives a flux $F_0(H\beta) = 1.85 \times 10^{-11}$ erg s⁻¹ cm⁻². The total flux for both components A and B is $F_0(H\beta) = 1.97 \times 10^{-11}$ erg s⁻¹ cm⁻². Thus, component B provides less than 10% of the total $H\beta$ energy. A Lyman continuum flux of $N_L = 2.10 \times 10^{49}$ photons s⁻¹ can be estimated for component A, using a distance of 66 kpc, if the H II region is ionization-bounded. A single O6V star can account for this ionizing flux (Vacca et al. 1996, Schaerer & de Koter 1997). Similarly, the Lyman

Fig. 1. A set of *HST* views of the SMC nebula N 88. (a) A “true-color” image of the whole WFPC2 field based on exposures taken with filters $H\alpha$ (red), $[O III]$ (green), and U (blue). (b) A False color image of the PC field in $H\alpha$. Field size $\sim 37'' \times 37''$ ($\sim 11 \times 11$ pc²). (c) A close-up of the $H\alpha$ image presented in Fig. 1b showing N 88A and its neighboring N 88B. Field size $\sim 12'' \times 12''$ ($\sim 3.5 \times 3.5$ pc²). The star lying towards N 88B is #55 (see text).

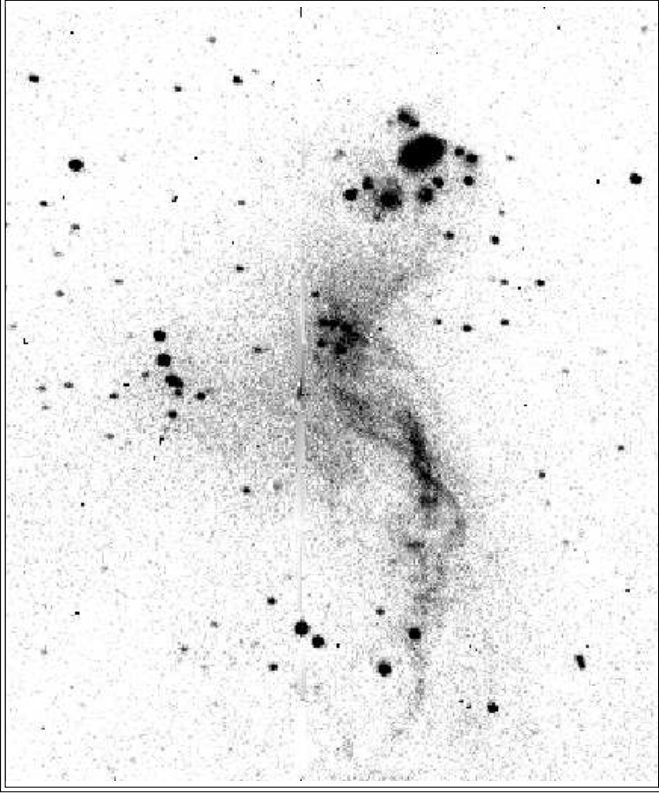


Fig. 2. A ground-based $H\alpha$ image of N 88 obtained with EFOSC attached to the ESO 3.6m telescope. Field size $\sim 1'.7 \times 2'.0$ (31×37 pc²). North is up and east is left. N 88A and B appear as the bright “blob” at the top of the image. Note the absence of ionized gas and stars north-west of the “blob”.

continuum flux corresponding to component B is $N_L \sim 3.5 \times 10^{47}$ photons s⁻¹. If we take the estimated UV fluxes at face values, the exciting star of component B should be an early B type star. However, these should be considered as lower limits, since the $H II$ regions are not ideally ionization-bounded.

We find an rms electron density of 2700 cm^{-3} for component A from the total $H\beta$ flux, a $T_e = 14000$ °K (Garnett et al. 1995), and assuming a radius of 0.5 pc for the object. The corresponding total ionized mass of N 88A is $\sim 45 M_\odot$.

The $[O III] \lambda 5007/H\beta$ intensity map displays an extended high excitation zone towards N 88A (Fig. 4b), where the ratio has a mean value of ~ 7 . The ratio peaks at some points to values as high as 9. Taking $T_e \sim 14000$ °K and $N_e = 2700 \text{ cm}^{-3}$, a ratio $[O III]/H\beta \sim 7$ indicates an ionic abundance $O^{++}/H^+ \sim 9.4 \times 10^{-5}$. Since the mean

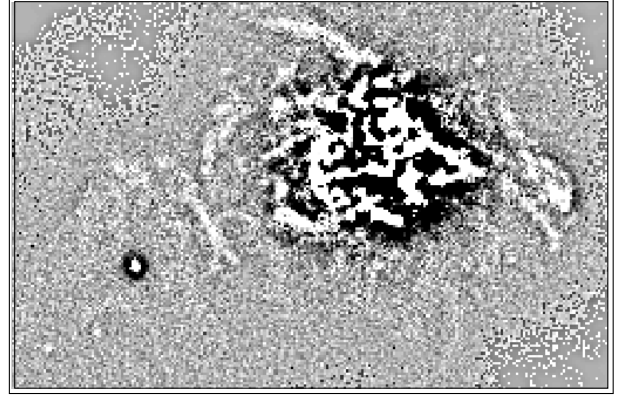


Fig. 3. An un-sharp masking $H\alpha$ image of N 88A & B which highlights the high spatial frequency filamentary patterns. Field size $\sim 11'' \times 7''.4$ (3.3×2.2 pc). North is up and east is left.

SMC oxygen abundance is $O/H \sim 10.5 \times 10^{-5}$ (Dufour 1984), this means that $\sim 90\%$ of the oxygen atoms in N 88A are in the form of doubly ionized O^{++} ions, in agreement with the result of Garnett et al. (1995). The $[O III]/H\beta$ ratio for component B is comparatively much smaller, with a mean value of ~ 4 .

The high excitation narrow filament emanating from component A is clearly visible in the $[O III]/H\beta$ map, suggesting that the O^{++} ions in the filament may be excited by shock collisions.

3.4. Stars

The *HST* images reveal tens of previously unknown stars towards the N 88 complex. Many of them, especially the brightest ones, are gathered in several small groups often un-resolved in the EFOSC image (Fig. 2). The photometry obtained for the 79 brightest stars of the field using the filters wide U (F300W), Strömgren v (F410M), Strömgren b (F467M), He II (F469N), and Strömgren y (F547) is presented in Table 1 which also gives the coordinates (J2000) of each star. These stars are identified by their numbers in Fig. 6 and Table 1. The capital letters in the last column of the table identify the associated $H II$ regions. The spectral types of the ionizing stars proposed by Wilcots (1994), as well as their labels, are also listed in the table. Note that the present observations show the exciting star of N 88D to be double (#71 & #72) and the given type corresponds therefore to both of them. Table 1 is available in electronic form at the Centre de Données astronomiques

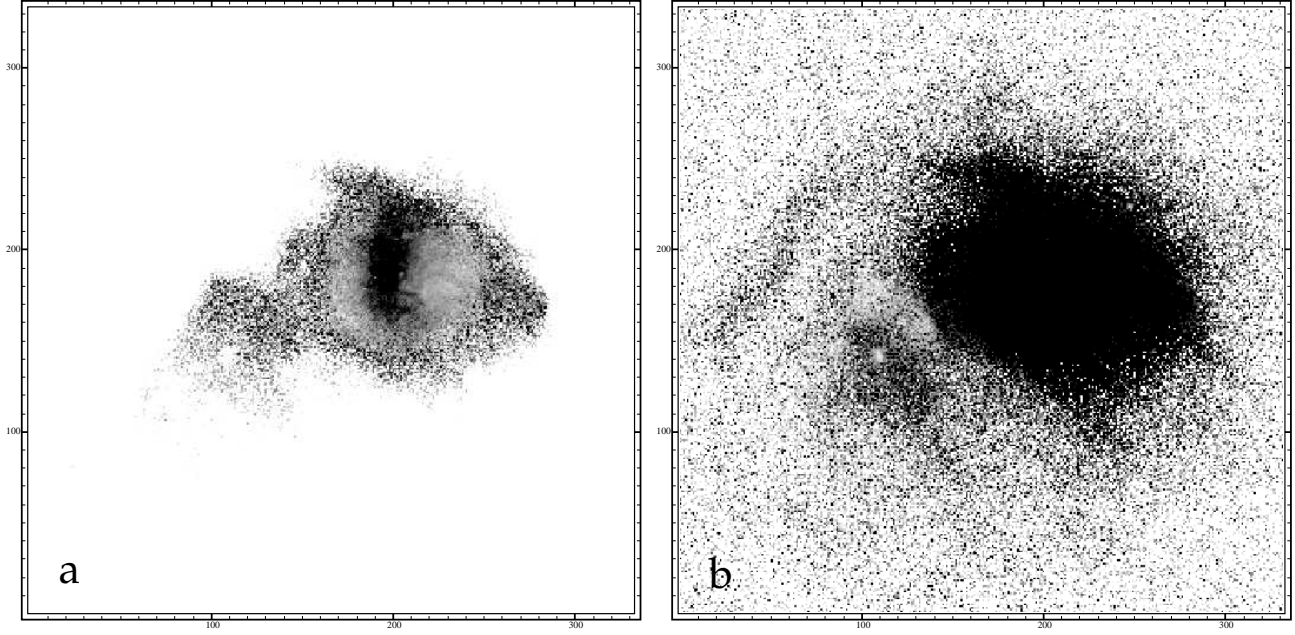


Fig. 4. Spatial variation in the extinction and ionization across N 88A. The field size ($13''.8 \times 13''.8$ or $\sim 4 \times 4$ pc) is almost identical to Fig. 1c. **(a)** Balmer $H\alpha/H\beta$ ratio of the inner parts of the nebulae. Darker color indicates higher $H\alpha/H\beta$. Note the presence of the narrow absorption lane where the extinction rises to $A_V \sim 3.5$ mag. The mean value of extinction towards component A is about 1.5 mag. **(b)** The $[O\text{ III}]/H\beta$ ratio. The mean value for component A is ~ 7 and the ratio rises to as high as 9 at some points. Note the narrow filament north-east of component B.

de Strasbourg (via anonymous ftp to cdsarc.u-strasbg.fr or via <http://cdsweb.u-strasbg.fr/Abstract.html>).

While the exciting stars of the fainter H II regions are easily identified on the true-color image, a remarkable point is the absence of prominent stars towards the main component A. Nevertheless, we detect two faint stars embedded in the core of N 88A east of the absorption lane (Fig. 5). These are stars #1 and #2 with $y = 18.2$ and 18.3 mag and colors $b - y = +0.9$ and $+0.6$ mag respectively. It should however be underlined that these magnitudes are very uncertain since the stars lie in a very bright area where nebular subtraction is not straightforward. A third fainter star ($y \sim 20$ mag), not visible in Fig. 5, is marginally detected just to the east of the bright $H\alpha$ core of N 88A. Its position suggests it as being a good candidate for an exciting star.

Star #55, situated towards the center of component B, has $y = 16.57$ mag and is one of the brightest in the field. It has a highly elongated PSF profile which is due to multiplicity (at least three components are resolved). This may be the star “s1” detected by Wilcots (1994) relatively close to the brightest part of N 88. Its spectrum shows strong $\text{He I } \lambda 4471 \text{ \AA}$ and $\text{He II } \lambda 4686$, but weak $\text{He II } \lambda 4541 \text{ \AA}$ indicative of an O9 V star. If this spectrum belongs actually to #55, it should correspond to the brightest component of this system.

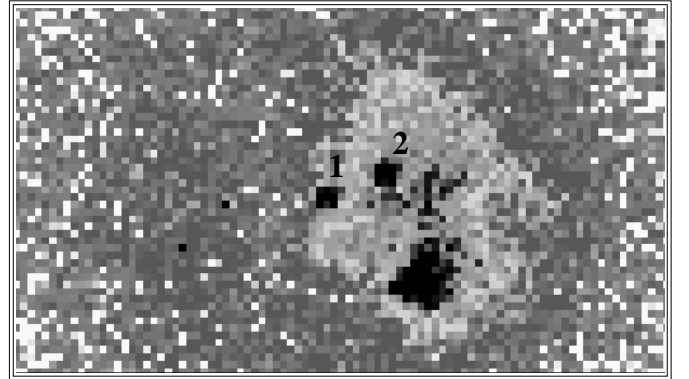


Fig. 5. The two stars lying towards the very bright inner part of N 88A (west of the absorption lane) are visible in this Strömgren y image (separated by $0''.4$, or ~ 0.1 pc). The dark spot south of the stars is the brightest core of N 88A. Field $\sim 4'' \times 2''$ ($\sim 1.2 \times 0.6$ pc 2). Same orientation as all other images.

The color-magnitude diagram for the brightest stars of the sample (Fig. 7) shows a main sequence with the bulk of the stars centered on Strömgren colors $b - y = -0.10$ and $v - b = -0.20$ mag, typical of massive OB stars (Relyea & Kurucz 1978). These colors are equivalent to a Johnson $B - V = -0.30$ (Turner 1990), which indicates a negligible

reddening (Conti et al. 1986). This result is due to the fact that the main sequence is overwhelmingly dominated by stars lying outside the N 88 complex and means that the areas situated north-east, east, south, and south-west of N 88 are not affected by dust.

However, taking a sub-sample made up of all the exciting stars of the N 88 H II regions (excluding stars #1 & #2), we find the Strömgren colors $b - y = 0.02$ and $v - b = -0.17$ which indicate $B - V = -0.21$ corresponding to a visual extinction of $A_V = 0.3$ mag. This clearly confirms that the N 88 complex is the most reddened part of this region of the SMC. Of particular interest are stars #60 and #61 situated immediately north-west of N 88A (Fig. 1b). Assuming that these two stars are of O type, their colors suggest an extinction of $A_V > 1$ mag. This result has implications for the location of the molecular cloud (Sect. 4.4).

The brightest stars of the sample are #39, #12, #19, and #6. The first two are blue stars and the latter ones are red. The red population showing up in the color-magnitude diagram represents a collection of evolved field stars as well as young massive ones contaminated by nebulousity/dust. For instance, it is noteworthy that the very red stars #76, and #74 are not associated with a nebulousity, and this suggests that they should be evolved field stars.

In the particular case of stars #1 and #2 lying inside N 88A, in spite of their red colors, they may be young blue stars suffering from heavy extinction. Assuming that star #1 has an O9 V spectrum with $M_V = -4.4$ mag (Vacca et al. 1996), and considering that the distance modulus of SMC is 19 mag, then an extinction of $A_V = 3.4$ mag is necessary to make it appear as faint as $y \sim 18$ mag. Similarly, in order for a star of spectral type O6 V (Sect. 3.3) to have an $y \sim 20$ mag, we need an $A_V \sim 6$ mag. Thus, the main exciting star(s) of N 88A should remain hidden in the optical due to the presence of dust by an extinction of at least 6 mag.

4. Discussion and concluding remarks

4.1. Comparison with N 81

The most striking feature of N 88A is its lack of prominent stars, even at the WFPC2 resolution. This indicates a young age and is supported by other observational findings about N 88A: its compactness, its high density, and its exceptionally high extinction. These facts considered together suggest that N 88A is just hatching from its natal molecular cloud. Stars #1 and #2 are probably among the exciting sources of N 88A. Other exciting stars may still be embedded in the densest part of the nebula, such as the bright spot highlighted in Fig. 1c and Fig. 5, and remain invisible due to the high dust content. Compared with N 81, N 88A is probably younger since N 81 is more extended, less dense, and exhibits several of its exciting stars

(Paper I). Although N 81 and N 88A are both very young, the present observations underline their difference. Apart from the exciting stars aspect, N 88A is surrounded by several diffuse H II regions. In contrast, N 81 is an isolated object. These facts point to the diversity of star forming regions belonging to the same chemical environment and also to the necessity of observing each case in detail.

On the other hand, the whole N 88 region is very reminiscent of the LMC N 59 region studied by Armand et al. (1992). N 88 and N 59 contain several individual H II regions, in various evolutionary states. They range from compact, bright and young components with a lot of dust hiding the exciting stars (N 88A and N 59A) to diffuse, spherical and evolved regions (N 88E-F-G-H and N 59C), and also to shell components (N 88B and N 59B which contains a supernova remnant). Similarly, both regions display a filamentary structure which results from the interaction of the strong stellar winds emitted by the massive stars with the surrounding medium, as well as small scale brightness variations pointing to a very inhomogeneous distribution of matter or dust inside or around these objects.

4.2. Associated neutral material

CO emission from the molecular cloud associated with N 88A was observed by Israel et al. (1993) using the ESO-SEST 15 m telescope. They detected the $^{12}\text{CO}(1-0)$ emission with a brightness temperature of 750 mK, a width of 2.5 km s^{-1} and a radial velocity of $V_{\text{LSR}} = 147.8 \text{ km s}^{-1}$. The molecular cloud is much brighter than the one associated with N 81 (Paper I) and ranks among the few sources in the SMC detected in $^{13}\text{CO}(1-0)$ (Israel et al. 1993). Rubio et al. (1996) mapped the molecular cloud in $^{12}\text{CO}(1-0)$ and $^{12}\text{CO}(2-1)$ transitions using the SEST telescope with respective spatial resolutions of $43''$ ($\sim 13 \text{ pc}$) and $22''$ ($\sim 7 \text{ pc}$). It turns out that the cloud is in fact relatively small, $\sim 1'$ (18 pc) in size in the east-west direction and slightly smaller in north-south. More recently, Rubio et al. (private communication) have detected molecular transitions $^{12}\text{CO}(3-2)$, CS(2-1), CS(3-2), $\text{HCO}^+(1-0)$ which probably originate from the hot and dense core of the cloud. Molecular hydrogen emission also has been detected towards N 88A (Israel & Koornneef 1988).

The SMC is known to have an overall complex structure with several overlapping neutral hydrogen layers (McGee & Newton 1981). We used the recent observations by Stanimirovic et al. (1998), with a resolution of $98''$ (30 pc), to examine the H I emission towards N 88. The H I spectrum profile has two main emission peaks at ~ 150 and $\sim 175 \text{ km s}^{-1}$. The column density corresponding to their sum is $3.12 \times 10^{21} \text{ atoms cm}^{-2}$, slightly smaller than that corresponding to N 81 (Paper I). It seems that the molecular cloud is correlated with the smaller velocity H I component.

Fig. 6. A finding chart indicating the brightest stars detected towards N 88, based on the WFPC2 He II image. The field of view is the same as in Fig. 1a. North is up and east is left. The photometry of those stars is presented in Table 1.

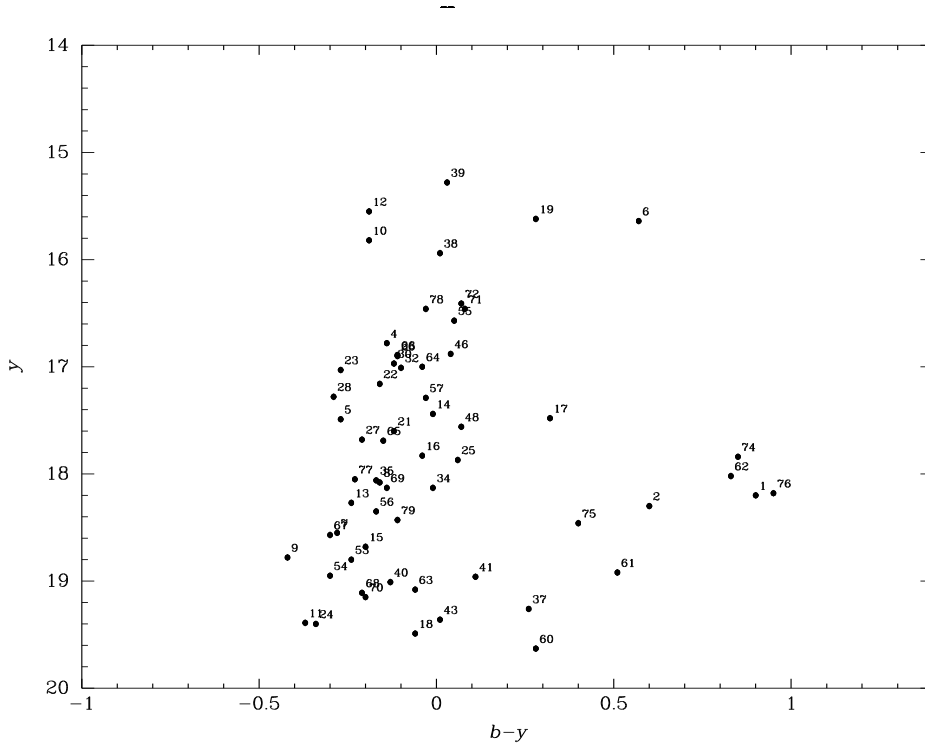


Fig. 7. Color-magnitude diagram, y versus $b-y$, of the brightest stars revealed towards the SMC compact H II region N 88. Numbers refer to Fig. 6 and Table 1.

4.3. Extinction

N 88 was detected as a very bright IRAS source (Schwering & Israel 1990). The fact that near infrared photometry of N 88A, at J , H , K , and L' bands obtained using a $10''$ aperture (Israel & Koornneef 1991), is consistent with the IRAS spectrum (12, 25, 60, and $100\,\mu\text{m}$) suggested that the IR emission arises mostly from the compact object in the aperture. Moreover, these authors found a quite red $K-L'$ color of more than 2 mag indicating the presence of hot dust.

Our *HST* images for the first time show the heavy concentration of absorbing dust towards the inner parts of the H II region. More strikingly, the extinction rises to as high as $A_V \sim 3.5$ mag in a narrow band towards the bright core of the nebula. This high absorption is quite unexpected for a metal-poor galaxy like the SMC. In fact N 88A holds the record of extinction among ionized nebulosities in the SMC. The correlation between the zones of the high excitation and high extinction is an argument in favor of the physical association of the dust with hot gas.

It is important to know the properties of this dust. Roche et al. (1987) studied $8-13\,\mu\text{m}$ spectra of N 88A and found a featureless continuum without any evidence of

dust signatures attributed to silicate grains. This led them to the conclusion that the dust is likely composed of carbon grains. Further progress in this area requires appropriate IR observations using the highest spatial resolutions.

4.4. Star formation

The N 88 nebular complex results from a small starburst which occurred recently in the Wing of the SMC. While the main stars creating N 88A are not visible, the other members of the starburst show up in the *HST* images (Fig. 1). The stars exciting the diffuse H II regions (C to H) were formed in the outer, less dense parts of the molecular cloud, whereas the compact, very dusty N 88A is associated with the core of this small molecular cloud (Sect. 4.2). The cloud must be to the north-east of N 88A, as indicated by the ionization front detected in that direction (Sect. 3.1) and also by the fact that stars #60 and #61 situated north of the front are heavily affected by extinction (Sect. 3.4). This is further supported by ground-based higher exposure images showing a large front north-west of N 88A beyond which no stars are visible (Fig. 2; also Testor & Pakull 1985).

The case of component B is interesting. Although it is, like N 88A, apparently related to the core of the molecular cloud, it seems more evolved. In fact N 88B has a significantly lower density and less dust, and reveals its exciting star (#55). It can be considered that N 88A has resulted from sequential star formation, that is the collapse of the shock/ionization front layer created by stars #55. If so, we are dealing with two successive generations of stars formed in the core of the molecular cloud.

The stars situated towards N 88 are also known as HW 81 following Hodge & Wright (1977) who surveyed the SMC in search of OB associations. The present observations reveal the fainter members of this association. The *HST* images also resolve another association in the direction of N 88. Lying $\sim 50''$ (15 pc) south-east of N 88A, at the lower-left corner of Fig. 1a, HW 82 (Hodge & Wright 1977) is composed of a dozen stars several of which are tightly packed multiple ones. HW 82 is not associated with ionized gas, and a relatively large number of its stars are red. At present we do not know whether the red and blue stars are co-spatial members of the same cluster. Nevertheless, the facts that the ionized gas is already dispersed from there and that no significant amount of dust is detected (Sect. 3.4) suggest that HW 82 represents an older burst of star formation in the Wing. This is confirmed by the larger field of EFOSC $H\alpha$ image (Fig. 2) which shows no H II regions south of the *HST* field of view. Star formation must have therefore proceeded from south to north and N 88 is the most recent site of star formation in this part of the SMC.

A noteworthy aspect of the stellar population towards N 88 is the presence of several tight clusters or multiple systems uncovered by the present observations. For example, the exciting star of N 88B (#55) is a multiple system of at least three components. There are also at least two stars hidden inside N 88A, while both N 88C and D are excited by two blue stars of comparable brightness. Note also the tight cluster in HW 82 composed of stars #9, #10, #11, #12, and #13. These cases present new pieces of evidence in support of collective formation of massive stars in the SMC (see Paper I for a brief discussion).

An intriguing, though unanswered question, is related to the origin of the large-scale filamentary veil visible in the EFOSC image. Our true-color image shows that filaments originating from north-east of N 88 run towards the anonymous blue cluster in the south (stars #16, #17, #21, #22, #23, and #24). However, the veil significantly brightens south of that cluster and bends to the south-east. In consequence, the association of the veil with the N 88 region is not established. It is possible that this filamentary structure is linked to the neighboring huge bubble nebula DEM 167 (Davies et al. 1976).

to acknowledge the financial support from a Marie Curie fellowship (TMR grant ERBFMBICT960967).

References

- Armand C., Deharveng L., Caplan J., 1992, A&A 265, 504
- Conti P.S., Garmany D., Massey P., 1986, AJ 92, 48
- Davies, R.D. Elliott K.H., Meaburn J., 1976, MNRAS 81, 89
- Dufour R.J., 1984, in Structure and Evolution of the Magellanic Clouds, eds. S. van den Bergh & K.S. de Boer, Reidel, Dordrecht, p. 353
- Dufour R.J., Harlow W.V., 1977, ApJ 216, 706
- Fruchter A.S., Hook R.N., 1998, PASP, submitted (astro-ph/9808087)
- Garnett D.R., Skillman, E.D., Dufour R.J., et al., 1995, ApJ 443, 64
- Henize K.G., 1956, ApJS 2, 315
- Heydari-Malayeri M., Beuzit J.-L., 1994, A&A 287, L17
- Heydari-Malayeri M., Testor G., 1982, A&A 111, L11
- Heydari-Malayeri M., Testor G., 1983, A&A 118, 116
- Heydari-Malayeri M., Testor G., 1985, A&A 144, 98
- Heydari-Malayeri M., Testor G., 1986, A&A 162, 180
- Heydari-Malayeri M., Le Bertre T., Magain P., 1988, A&A 195, 230
- Heydari-Malayeri M., Van Drom E., Leisy P., 1990, A&A 240, 481
- Heydari-Malayeri M., Rosa M.R., Zinnecker H., Deharveng L., Charmandaris V., 1999, A&A 344, 848 (Paper I)
- Hodge P.W., Wright F.W., 1977, *The Small Magellanic Cloud* (Seattle: University of Washington Press)
- Israel F. P., Koornneef J., 1988, A&A 190, 21
- Israel F. P., Koornneef J., 1991, A&A 248, 404
- Israel F.P., Johansson L.E.B., Lequeux J., et al., 1993, A&A 276, 25
- Kurt C.M., Dufour J., Garnett E.D., et al., 1995, RexMexAA 3, 223
- McGee R.X., Newton L.M., 1981, Proc. Astron. Soc. Australia 4, 189
- Prévot M.L., Lequeux J., Maurice E., Prévot L., Rocca-Volmerange B., 1984, A&A 132, 389
- Relyea L.J., Kurucz R.L., 1978, ApJS 37, 45
- Roche P.F., Aitken D.K., Smith C.H., 1987, MNRAS 228, 269
- Rubio M., Lequeux J., Boulanger F., et al., 1996, A&AS 118, 263
- Schaerer D., de Koter A., 1997, A&A 322, 598
- Schwing P.B.W., Israel F.P., 1990, Atlas and Catalogue of Infrared Sources in the Magellanic Clouds, Kluwer, Dordrecht
- Stanimirovic S., Stavley-Smith L., Dickey J.M., et al., 1998, MNRAS, in press
- Testor, G. Pakull M., 1985, A&A 145, 170
- Turner D.G., 1990, PASP 102, 1331
- Vacca W.D., Garmany C.D., Shull J.M., 1996, ApJ 460, 914
- Wilcots E.M., 1994, AJ 108, 1674

Acknowledgements. We are grateful to an anonymous referee for his careful reading of the manuscript and comments that contributed to substantially improve the paper. VC would like

Table 1. Photometry of the brightest stars towards N 88

Star	α (J2000)	δ (J2000)	wide U (F300W)	v (F410M)	b (F467M)	He II (F469N)	y (F547M)	Notes [†]
1	1:24:08.10	-73:09:03.98	—	—	19.1	—	18.2	
2	1:24:08.02	-73:09:03.84	—	—	18.9	—	18.3	
4	1:24:25.42	-73:10:25.20	14.83	16.35	16.64	16.70	16.78	
5	1:24:27.12	-73:10:24.20	15.56	17.10	17.22	17.14	17.49	
6	1:24:27.58	-73:10:19.97	16.82	16.94	16.21	16.27	15.64	
7	1:24:27.39	-73:10:19.50	16.84	18.21	18.27	18.42	18.55	
8	1:23:57.75	-73:10:17.77	16.51	17.74	17.92	17.95	18.08	
9	1:24:28.00	-73:10:15.11	16.97	18.19	18.36	18.59	18.78	
10	1:24:28.29	-73:10:13.63	13.54	15.34	15.63	15.73	15.82	
11	1:24:27.83	-73:10:13.06	17.91	18.92	19.02	19.30	19.39	
12	1:24:28.23	-73:10:12.98	13.39	15.14	15.36	15.42	15.55	
13	1:24:28.09	-73:10:12.39	16.42	17.86	18.03	17.92	18.27	
14	1:24:21.08	-73:10:10.12	15.86	17.33	17.43	17.47	17.44	
15	1:24:20.38	-73:10:10.01	17.32	18.36	18.48	18.54	18.68	
16	1:24:14.68	-73:10:10.16	16.19	17.62	17.79	17.89	17.83	
17	1:24:16.27	-73:10:08.28	18.52	18.28	17.80	17.76	17.48	
18	1:24:26.37	-73:10:06.22	18.91	19.43	19.43	19.80	19.49	
19	1:24:28.52	-73:10:05.18	16.25	16.19	15.90	15.98	15.62	
21	1:24:14.42	-73:10:03.10	15.77	17.34	17.48	17.49	17.60	
22	1:24:15.30	-73:10:01.91	15.29	16.89	17.00	17.10	17.16	
23	1:24:16.08	-73:10:01.38	14.96	16.60	16.76	16.93	17.03	
24	1:24:13.82	-73:10:01.50	17.72	18.98	19.06	19.30	19.40	
25	1:24:07.39	-73:10:01.03	16.47	17.71	17.93	17.93	17.87	
26	1:23:59.63	-73:09:48.58	15.06	16.63	16.79	16.77	16.90	
27	1:24:02.37	-73:09:48.20	15.72	17.35	17.47	17.57	17.68	
28	1:24:22.40	-73:09:43.50	15.40	16.82	16.99	17.19	17.28	
30	1:24:03.05	-73:09:34.47	15.30	16.65	16.85	16.82	16.97	
32	1:24:06.48	-73:09:32.96	15.20	16.80	16.91	16.94	17.01	
34	1:24:11.99	-73:09:26.63	16.74	18.11	18.12	18.14	18.13	
35	1:24:02.55	-73:09:25.42	16.70	17.87	17.89	17.98	18.06	
37	1:24:07.62	-73:09:21.20	18.97	19.50	19.52	19.71	19.26	
38	1:24:11.09	-73:09:20.59	14.20	15.72	15.95	15.89	15.94	H (B0 III, s3)
39	1:24:13.94	-73:09:19.47	13.39	14.98	15.31	15.30	15.28	
40	1:24:27.56	-73:09:17.94	17.72	18.89	18.88	18.99	19.01	
41	1:24:08.69	-73:09:19.24	18.15	18.53	19.07	19.06	18.96	
43	1:24:07.69	-73:09:17.90	18.01	18.92	19.37	19.14	19.36	
46	1:24:07.21	-73:09:15.60	15.25	16.63	16.92	16.81	16.88	C
48	1:24:07.37	-73:09:14.63	15.88	17.32	17.63	17.54	17.56	C
53	1:24:20.76	-73:09:08.05	17.75	18.41	18.57	18.63	18.81	
54	1:24:15.05	-73:09:06.80	17.39	18.21	18.65	18.68	18.95	
55	1:24:09.09	-73:09:06.05	15.21	16.57	16.62	16.62	16.57	B
56	1:24:14.64	-73:09:05.42	16.91	18.08	18.18	18.30	18.35	
57	1:24:05.66	-73:09:05.06	15.50	16.97	17.26	17.26	17.29	F
60	1:24:07.65	-73:09:02.22	18.51	19.83	19.91	19.33	19.63	
61	1:24:06.91	-73:09:01.67	17.87	19.04	19.43	18.85	18.92	
62	1:24:09.05	-73:08:55.90	—	19.70	18.85	18.54	18.02	
63	1:24:10.88	-73:08:55.38	17.78	18.86	19.02	18.79	19.08	
64	1:24:09.88	-73:08:53.65	15.49	16.86	16.96	16.95	17.00	G (O9.5 I, #4)
65	1:24:26.97	-73:08:44.10	15.74	17.28	17.54	17.46	17.69	
66	1:24:22.46	-73:08:41.42	15.29	16.52	16.78	16.76	16.89	
67	1:24:13.95	-73:08:36.73	17.21	18.29	18.27	18.51	18.57	
68	1:24:17.58	-73:08:29.33	18.48	19.37	18.90	19.58	19.11	
69	1:24:24.35	-73:08:28.14	16.26	17.75	17.99	18.03	18.13	
70	1:24:16.32	-73:08:14.91	17.74	18.53	18.95	18.66	19.15	
71	1:24:04.97	-73:09:15.11	15.05	16.55	16.54	16.46	16.46	D (B0 III, #6)
72	1:24:04.97	-73:09:14.38	14.97	16.42	16.48	16.31	16.41	D
73	1:24:04.80	-73:09:07.55	—	—	—	—	—	E (B0 V, #5)
74	1:24:05.23	-73:10:03.39	20.42	19.96	18.69	18.52	17.84	

Table 1. (continued)

Star	α (J2000)	δ (J2000)	wide U (F300W)	v (F410M)	b (F467M)	He II (F469N)	y (F547M)	Notes [†]
75	1:24:02.35	-73:10:01.49	19.65	19.23	18.86	18.94	18.46	
76	1:24:27.49	-73:10:31.19	22.46	20.12	19.13	18.96	18.18	
77	1:24:29.48	-73:10:17.94	16.24	17.70	17.82	17.94	18.05	
78	1:24:12.68	-73:09:16.29	14.65	16.20	16.43	16.46	16.46	
79	1:24:12.71	-73:09:13.91	16.92	18.14	18.32	18.42	18.43	

[†] The capital letters B to H indicate the associated H II regions presented in Fig. 1b. The spectral types and identifications of Wilcots (1994) for some stars are included inside parentheses.